JOURNAL OF SOLID STATE CHEMISTRY **136,** 181–192 (1998)
ARTICLE NO. SC977673

Structural Investigations of Ammonium Vanadium Diphosphates by X-Ray Powder Diffraction

J. Trommer,[1] H. Worzala, S. Rabe, and M. Schneider

Institut für Angewandte Chemie Berlin—Adlershof e.V., Rudower Chaussee 5, D-12484 Berlin, Germany

Received May 1, 1997; in revised form October 17, 1997; accepted October 23, 1997

The crystal structures of three ammonium vanadium diphosphates have been investigated by means of X-ray powder diffraction including ab initio structure determination and Rietveld refinement. The compound $NH_4VP_2O_7$ crystallizes in the monoclinic space group $P2_1/c$ with $a = 7.5149(2)$ Å, $b = 10.0384(3)$ Å, $c = 8.2422(2)$ Å, $\beta = 105.988(3)^\circ$, and $Z = 4$. The two ammonium vanadyl diphosphates are $(NH_4)_2VOP_2O_7$, which has a tetragonal unit cell, space group $P4bm$, $a = 8.3039(2)$ Å, $c = 5.7658(2)$ Å, and $Z = 2$, and α-$(NH_4)_2(VO)_3(P_2O_7)_2$, which has an orthorhombic structure, space group $Pnam$, $a = 17.4973(4)$ Å, $b = 11.3655(3)$ Å, $c = 7.2769(2)$ Å, and $Z = 4$. The first and the third structures consist of a framework of corner-sharing VO_x polyhedra and PO_4 tetrahedra and intersecting channels, whereas $(NH_4)_2VOP_2O_7$ is arranged in layers built-up from VO_5 square pyramids and P_2O_7 groups and the NH_4^+ cations in between. The three NH_4 compounds are isostructural to the equivalent alkali vanadium diphosphates. © 1998 Academic Press

INTRODUCTION

Vanadium phosphates are used as catalysts and as precursors for catalysts in reactions such as the oxidation of *n*-butane to maleic anhydride (1) and the ammoxidation of substituted methylaromatics (2, 3) and heteroaromatics (4) into nitriles. In the latter case under ammoxidation conditions (ammonia, air, water vapor, and with or without a methylaromatic), various precursor compounds of the vanadium phosphates (α- and β-$VOPO_4$, $VOHPO_4 \cdot 0.5H_2O$, $VOHPO_4$) are transformed and α-$(NH_4)_2(VO)_3(P_2O_7)_2$ is found as major phase (2, 5, 6). Beside the generation of this ammonium vanadyl diphosphate during the ammoxidation, the phase can also be synthesized directly by heating a mixture of V_2O_5 and $(NH_4)_2HPO_4$(5).

Another ammonium vanadyl diphosphate, $(NH_4)_2VOP_2O_7$, was also used as a precursor for investigations of the ammoxidation of aromatic compounds; in this case the transformation proceeded mainly into the phase $NH_4VP_2O_7$ (2). Both ammonium phases can be synthesized from the same components as mentioned above. Until now none of these structures has been ascertained. From a comparative analysis (5, 6) of preliminary crystal data, such as lattice constants, space group, etc., it has been assumed that there is a structural relationship to known alkali compounds: MVP_2O_7 (7–9), $M_2VOP_2O_7$ (10), $M_2(VO)_3(P_2O_7)_2$ (11–13) (M = K, Rb, Cs).

Structure models for the ammonium vanadium phosphates would help us obtain better insight into the observed phase transformations of the precursors to the actual active catalysts under ammoxidation conditions.

The synthesis of these substances gave no single crystals suitable for a structure determination in the usual way using single crystal methods. The size of the crystallites did not exceed 30 μm in diameter, therefore powder diffraction methods had to be applied including new developments such as pattern decomposition, ab initio structure solution, and refinement, the latter based on the Rietveld technique (14). This approach has already been applied successfully for the structure determination in the field of vanadium phosphates such as α- and β-$VOHPO_4 \cdot 2H_2O$ (15, 16) and $(VO)_3(PO_4)_2 \cdot 9H_2O$ (17).

In the present work we describe the crystal structures of the three ammonium vanadium phosphates as mentioned above. Their structural analysis is based on laboratory powder diffraction data collected on a transmission powder diffractometer (Debye–Scherrer geometry). For the purpose of comparison, $NH_4VP_2O_7$ was also measured on a Bragg–Brentano diffractometer.

EXPERIMENTAL

All three ammonium vanadium diphosphates have been synthesized from mixtures, containing V_2O_5 and $(NH_4)_2HPO_4$ of analytical grade, under different heating conditions. For the preparation of $NH_4VP_2O_7$ a mixture with a V : P : N mole ratio of 1 : 4 : 8 was heated up to 633 K for about 10 h. The obtained product, a green powder, was

[1]To whom correspondence should be addressed.

0022-4596/98 $25.00

then leached with 50% concentrated HCl, washed with water, and dried in air. In the case of ammonium vanadium(IV) diphosphates, $(NH_4)_2VOP_2O_7$ was obtained from a V : P : N mole ratio of 1 : 6 : 12 at a temperature of about 553 K, whereas α-$(NH_4)_2(VO)_3(P_2O_7)_2$ was synthesized from a mixture with V : P : N of 1 : 8 : 16 at 598 K for at least 2 h (normally about 10 h) in air (5, 18). The light green powders were eluted with water and dried in air.

All samples were measured on a STADI P automated transmission diffractometer from STOE with an incident beam curved germanium monochromator selecting Cu$K\alpha_1$ radiation and a 6° linear position sensitive detector (PSD). The alignment was checked by use of a silicon standard. For the Rietveld refinement and pattern decomposition, the samples were filled in glass capillaries with 0.3 mm in diameter and rotated during the data collections. Details of the measurements are given in the Tables 1, 3, and 5.

The additional data collection for $NH_4VP_2O_7$ using the Bragg–Brentano geometry was carried out on a SIEMENS D500. Its setup comprises a curved quartz crystal monochromator in the incident beam to select Cu$K\alpha_1$ radiation and a scintillation detector with a slit of 0.05° divergence in front of it. Measurement details are given in Table 1. The sample was ground and backpacked to reduce orientation effects and rotated during the data collection.

RESULTS AND DISCUSSION

Data Analysis of $NH_4VP_2O_7$

The basic crystallographic data (lattice constants, space group) of the compound $NH_4VP_2O_7$ were determined using the program suite VISUAL X^{POW} by STOE & CIE (20) and are given in Table 1. From the systematic absences ($h0l$, $l = 2n + 1$ and $0k0$, $k = 2n + 1$), the space group $P2_1/c$ could be ascertained unequivocally. A comparison with the unit cells of the known compounds MVP_2O_7 (M = K, Rb, Cs) (7–9) indicated that they are structurally related to each other.

The data, collected on the STOE STADI P, were decomposed in 689 individual reflection intensities by means of the Le Bail method (21) using the program PROFIL (22). This pattern fitting without a structural model led to the profile R factor, background excluded, $R_{wp} = 11.1\%$ with $R_{exp} = 7.8\%$. A straightforward attempt to determine the structure with the program SHELXS-86 (23) using the first 299 observable reflections as input gave no satisfactory solution. Therefore the structure of KVP_2O_7 was used as the starting model for a Rietveld refinement with the program PROFIL using the data sets from the STOE STADI P and the Siemens D500. Details about both refinements are given in Table 1, and it shows that the results are comparable. Differences in the lattice constants, caused by possible systematic errors (24) due to aberrations in the diffractometer geometry, indicate that the calculated standard deviations are an order of magnitude too small. The profile fit using the Siemens D500 data set is slightly better than that of the STOE STADI P expressed by the ratio R_{wp}/R_{exp}. The difference between the R_{wp} and R_{exp} factors, background excluded, and the residuals with the included background are not significant for the Bragg–Brentano data. In the transmission case the more realistic profile R value with respect

TABLE 1
Parameters of the Rietveld Refinement of $NH_4VP_2O_7$, Comparison of Measurements on STOE STADI P and Siemens D500 Diffractometers Using Cu$K\alpha_1$ Radiation

	STOE STADI P Debye–Scherrer geometry, 0.3 mm capillary[a]	Stemens D500 Bragg–Brentano geometry
2θ range (deg), step size (deg)	10.00–90.00, 0.02	10.00–90.00, 0.02
Counting time per step (s)	3900	20
Zero-point error (deg)	− 0.0021(6)	− 0.0209(9)
Crystal symmetry	Monoclinic	Monoclinic
Space group, Z	$P2_1/c$, 4	$P2_1/c$, 4
Cell parameters		
a (Å)	7.5149(2)	7.5164(3)
b (Å)	10.0384(3)	10.0317(3)
c (Å)	8.2422(2)	8.2414(3)
β (°)	105.988(3)	105.969(3)
V_c (Å^3)	597.72(4)	597.43(5)
Formula weight	242.92	242.92
Calc. density ρ (g/cm^3)	2.70	2.70
FWHM (deg) (halfwidth parameters)		
U	0.070(7)	0.077(9)
V	− 0.035(4)	− 0.011(5)
W	0.0139(7)	0.064(6)
Profile shape function	Pseudo-Voigt	Pseudo-Voigt
Lorentz fraction η	0.41(1)	0.211(7)
Asymmetry	1.00 fixed	6.4(1.8)
No. of contributing Bragg reflections	484	483
Total no. of parameters	59	60
No. of structural parameters (+ restraints[b])	49(10)	49(10)
Profile R factors (%)		
Background excluded[c]	$R_{wp} = 12.5$, $R_{exp} = 7.5$	$R_{wp} = 13.4$, $R_{exp} = 10.1$
Background included[d]	$R_{wp} = 5.7$, $R_{exp} = 4.3$	$R_{wp} = 11.3$, $R_{exp} = 10.0$
Intensity R factor (%)	$R_I = 6.2$	$R_I = 5.5$

[a]Absorption correction for a 0.3 mm capillary, packing density (estimated from beam attenuation measurements) of about 56%, $\mu = 10.70\,mm^{-1}$.

[b]Restraints were used to fix calculated H atom positions around the N atom, forming an NH_4^+ cation tetrahedron.

[c]Weights w_i are calculated according to $w = 1/[Y(\text{total}) + \text{background}]$, where the background was interpolated by user defined points.

[d]Profile R factor as calculated with the computer program DBW et seq. by D. Wiles and R. Young (19).

to the intensity R factor (Bragg R factor) is calculated by excluding the high background of the pattern.

The positional parameters of the structural models obtained from both data sets differ mostly within their standard deviations. On the other hand, the errors in the positions are a magnitude higher than those normally calculated from single crystal data, e.g. compared to the isostructural compounds MVP_2O_7 with M = K, Rb, Cs (7–9).

Differences in the thermal parameters between the two derived structure models (data sets measured in Debye–Scherrer and Bragg–Brentano mode) as given in Table 2 are caused by their geometries and by the mainly inadequate correction of effects such as absorption in the transmission case (25). Generally, the determination of displacement parameters of polycrystalline materials with X-rays is limited by several factors, e.g. falloff of the atomic scattering factors with the diffraction angle, difficulties in the background determination because of the peak overlap in the higher 2θ range, problems with the peak shape modeling, and the limited 2θ range.

TABLE 2
Site Symmetries, Final Positional and Displacement Parameters, and Number (N) of Atoms per Unit Cell for $NH_4VP_2O_7$

Atom	Site symmetry	x^a	y^a	z^a	B_{iso}(Å^2)^{a,b}	N
V	4 × 1	0.241(1)	0.1007(6)	0.2588(8)	0.5(1)	4
		0.242(1)	0.1020(7)	0.262(1)	0.3(2)	
N	4 × 1	0.810(3)	0.187(1)	0.448(3)	1.3(6)	4
		0.821(4)	0.188(2)	0.456(4)	2.6(9)	
P(1)	4 × 1	0.131(1)	0.404(1)	0.332(1)	0.4(1)	4
		0.128(2)	0.406(1)	0.330(1)	0.5(2)	
P(2)	4 × 1	0.435(1)	0.3654(9)	0.188(1)	0.4(1)	4
		0.434(2)	0.365(1)	0.188(1)	0.5(2)	
O(1)	4 × 1	0.148(3)	0.088(2)	0.015(2)	0.2(2)	4
		0.147(3)	0.089(2)	0.016(3)	0.3(2)	
O(2)	4 × 1	0.323(2)	0.103(2)	0.514(2)	0.2(2)	4
		0.324(3)	0.107(2)	0.509(3)	0.3(2)	
O(3)	4 × 1	0.005(2)	0.001(2)	0.277(2)	0.2(2)	4
		0.002(3)	0.003(2)	0.277(3)	0.3(2)	
O(4)	4 × 1	0.446(2)	0.222(2)	0.238(2)	0.2(2)	4
		0.446(3)	0.220(2)	0.236(3)	0.3(2)	
O(5)	4 × 1	0.372(2)	−0.070(2)	0.267(2)	0.2(2)	4
		0.374(3)	−0.069(2)	0.273(3)	0.3(2)	
O(6)	4 × 1	0.088(2)	0.266(2)	0.259(3)	0.2(2)	4
		0.091(3)	0.265(2)	0.264(3)	0.3(2)	
O(7)	4 × 1	0.330(2)	0.442(2)	0.311(2)	0.2(2)	4
		0.331(3)	0.447(2)	0.311(3)	0.3(2)	
H(1)^c	4 × 1	0.76(2)	0.280(7)	0.46(2)	1.6	4
		0.74(1)	0.27(2)	0.47(3)	3	
H(2)^c	4 × 1	0.74(2)	0.12(1)	0.50(2)	1.6	4
		0.81(4)	0.11(1)	0.53(3)	3	
H(3)^c	4 × 1	0.948(8)	0.18(2)	0.51(2)	1.6	4
		0.96(1)	0.22(2)	0.49(3)	3	
H(4)^c	4 × 1	0.79(3)	0.17(2)	0.322(7)	1.6	4
		0.78(4)	0.16(2)	0.33(1)	3	

[a] Positional and displacement parameters: (1) line refinement with data from STOE STADI P; (2) line with data from Siemens D500.

[b] Displacement parameters were refined in groups depending on the atom type, and the B values of the hydrogen atoms were fixed.

[c] Positions of the hydrogen atoms are calculated using geometrical restraints for a NH_4^+ tetrahedron. N–H distance, 1.03 Å; H–N–H angle, 109.5° ("International Tables for X-ray Crystallography" (25)).

TABLE 3
Parameters of the Rietveld Refinement of $(NH_4)_2VOP_2O_7$, Data Measured on a STOE STADI P Diffractometer with Cu$K\alpha_1$ Radiation (Debye–Scherrer Geometry, 0.3 mm Capillary[a])

2θ range (deg), step size (deg)	5.00–100.00, 0.02
Counting time per step (s)	3900
Zero-point error (deg)	0.0050(7)
Crystal symmetry	tetragonal
Space group, Z	$P4bm$, 2
Cell parameters	
a (Å)	8.3039(2)
b (Å)	8.3039(2)
c (Å)	5.7658(2)
V_c (Å^3)	397.58(2)
Formula weight	276.96
Calc. density ρ (g/cm^3)	2.31
FWHM (deg) (halfwidth parameters)	
U	0.033(5)
V	−0.024(4)
W	0.0120(6)
Profile shape function	Pseudo-Voigt
Lorentz fraction η	0.36(2)
Asymmetry	1.00 fixed
No. of contributing Bragg reflections	130
Total no. of parameters	30
No. of structural parameters (+ restraints[b])	22(6)
Profile R factors (%)	
Background excluded[c]	R_{wp} = 14.4, R_{exp} = 5.4
Background included[d]	R_{wp} = 6.20, R_{exp} = 4.2
Intensity R factor (%)	R_I = 5.8

[a] No absorption correction for a 0.3 mm capillary, no significant beam attenuation observed. $\mu_{theoret}$ = 14.61 mm^{-1} (100% packing density).

[b,c,d] See footnotes to Table 1.

The structure refinement of $NH_4VP_2O_7$ with all non-hydrogen positions led for both data sets (absorption correction in the transmission case) to a negative displacement factor B for nitrogen; thus the thermal parameters were refined in groups according to atom type as given in Table 2. This effect was also observed after refining the other two ammonium vanadium diphosphates, whose structures will be described later.

Therefore it was assumed that this effect was not caused by possible systematic errors in the data but by deficiencies in the model, i.e. missing the hydrogen positions of the NH_4^+ cation. Theoretical calculations of the H atom positions by applying chemical restraints on distances and angles to form a NH_4^+ tetrahedron (26) during the refinement with

TABLE 4

Site Symmetries, Final Positional and Displacement Parameters, and Number (*N*) of Atoms per Unit Cell for $(NH_4)_2VOP_2O_7$

Atom	Site symmetry	*x*	*y*	*z*	B_{iso} (Å^2)[b]	*N*
V	$2\times4..$	0	0	0.1	1.2(2)	2
N	$4\times..m$	0.326(2)	0.174(2)	− 0.389(5)	2.0(5)	4
P	$4\times..m$	0.1278(7)	0.3722(7)	0.107(4)	0.9(2)	4
O(1)	$2\times4..$	0	0	0.380(4)	2.0(3)	2
O(2)	$4\times..m$	0.129(2)	0.371(2)	0.368(5)	2.0(3)	4
O(3)	8×1	0.071(2)	0.217(2)	0.001(3)	2.0(3)	8
O(4)	$2\times..mm$	0	1/2	0.009(4)	2.0(3)	2
H(1)[c]	$4\times..m$	0.404(4)	0.096(4)	− 0.31(1)	2.5	4
H(1A)[c]	$4\times..m$	0.262(7)	0.238(7)	− 0.27(2)	2.5	4
H(2)[c]	8×1	0.25(1)	0.109(3)	− 0.49(2)	2.5	8

[b,c]See corresponding footnotes in Table 2.

PROFIL (22) resulted in a better structural fit, i.e. the intensity *R* factor, R_1, dropped from around 8.8% down to 6.2% and the profile *R* factors also improved slightly. The thermal parameter for N was now positive and comparable to the values of the cations in the isostructural alkali compounds. The displacement factor for the hydrogen atoms was fixed at about 1.2–1.3 times the value of nitrogen.

The same procedure was also applied to the two ammonium vanadyl diphosphates as given in the Tables 4 and 6.

The final structural parameters for $NH_4VP_2O_7$ from the Rietveld refinement (convergence criterion: the maximum shift/error value is smaller than 0.10 or 10%) are given in Table 2. The final Rietveld refinement plot for both data sets is displayed in Fig. 1.

TABLE 5

Parameters of the Rietveld Refinement of α-$(NH_4)_2(VO)_3(P_2O_7)_2$, Data Measured on a STOE STADI P Diffractometer with Cu*K*α$_1$ Radiation (Debye–Scherrer Geometry, 0.3 mm capillary[a])

2θ range (deg), step size (deg)	5.00–90.00, 0.02
Counting time per step (s)	3900
Zero-point error (deg)	− 0.0092(5)
Crystal symmetry	Orthorhombic
Space group, *Z*	*Pnam*[e], 4
Cell parameters	
a (Å)	17.4973(4)
b (Å)	11.3655(3)
c (Å)	7.2769(2)
V_c (Å^3)	1447.13(8)
Formula weight	584.78
Calc. density ρ (g/cm^3)	2.68
FWHM (deg) (half-width parameters)	
U	0.089(7)
V	− 0.051(4)
W	0.0211(6)
Profile shape function	Pseudo-Voigt
Lorentz fraction η	0.41(1)
Asymmetry	1.00 fixed
Number of contributing Bragg reflections	672
Total no. of parameters	72
No. of structural parameters (+ restraints[b])	63(19)
Profile *R* factors (%)	
Background excluded[c]	$R_{wp} = 9.0$, $R_{exp} = 6.5$
Background included[d]	$R_{wp} = 2.3$, $R_{exp} = 1.6$
Intensity *R*-factor (%)	$R_I = 7.3$

[a]Absorption correction for a 0.3 mm capillary, packing density (estimated from beam attenuation measurements) of about 38%, $\mu = 8.03\,mm^{-1}$.

[b,c,d] See footnotes to Table 1.

[e]Standard setting was *Pnma*. The above setting was chosen to keep it in relation with the known isostructural compound α-$K_2(VO)_3(P_2O_7)_2$.

Data Analysis of $(NH_4)_2VOP_2O_7$

The compound $(NH_4)_2VOP_2O_7$ was measured on the transmission diffractometer STOE STADI P, and preliminary crystal data (Table 3) were determined using the program package VISUAL X^{POW} (20) as mentioned in the previous section. The determined lattice constants, crystal system (tetragonal), and the systematic absences (*P*–/–*b*–)

TABLE 6

Site Symmetries, Final Positional and Displacement Parameters, and Number (*N*) of Atoms per Unit Cell for $(NH_4)_2(VO)_3(P_2O_7)_2$

Atom	Site Symmetry	*x*	*y*	*z*	B_{iso} (Å^2)[b]	*N*
V(1)	$4\times..m$	0.4007(4)	0.6613(6)	1/4	1.0(1)	4
V(2)	$4\times..m$	0.3107(3)	0.3370(7)	1/4	1.0(1)	4
V(3)[d]	8×1	0.498(1)	0.003(2)	0.032(2)	1.0(1)	4
N(1)	$4\times..m$	0.358(1)	0.529(2)	3/4	3.5(6)	4
N(2)	$4\times..m$	0.326(1)	0.143(2)	3/4	3.5(6)	4
P(1)	8×1	0.1725(4)	0.3898(6)	0.5464(9)	0.5(1)	8
P(2)	8×1	0.4707(4)	0.2917(5)	0.046(1)	0.5(1)	8
O(1)	8×1	0.3501(8)	0.761(1)	0.439(2)	0.8(1)	8
O(2)	$4\times..m$	0.193(1)	0.434(2)	3/4	0.8(1)	4
O(3)	8×1	0.2475(8)	0.406(1)	0.447(2)	0.8(1)	8
O(4)	8×1	0.3910(8)	0.338(1)	0.439(2)	0.8(1)	8
O(5)	8×1	0.4777(8)	0.628(1)	0.433(2)	0.8(1)	8
O(6)	$4\times..m$	0.505(1)	0.295(2)	1/4	0.8(1)	4
O(7)	8×1	0.3888(7)	− 0.036(1)	0.973(2)	0.8(1)	8
O(8)	8×1	0.4730(7)	0.171(1)	0.975(2)	0.8(1)	8
O(9)	$4\times..m$	0.487(1)	0.010(2)	1/4	0.8(1)	4
O(10)	$4\times..m$	0.343(1)	0.551(2)	1/4	0.8(1)	4
O(11)	$4\times..m$	0.276(1)	0.206(2)	1/4	0.8(1)	4
H(1A)[c]	$4\times..m$	0.303(5)	0.50(2)	3/4	4	4
H(1B)[c]	$4\times..m$	0.36(1)	0.620(3)	3/4	4	4
H(1C)[c]	8×1	0.387(5)	0.50(1)	0.866(2)	4	8
H(2A)[c]	$4\times..m$	0.30(1)	0.06(1)	3/4	4	4
H(2B)[c]	$4\times..m$	0.29(1)	0.21(2)	3/4	4	4
H(2C)[c]	8×1	0.360(1)	0.15(1)	0.866(2)	4	8

[b,c]See corresponding footnotes in Table 2.

[d]Disorder in the V(3) atomic position and displacement from the inversion center were observed.

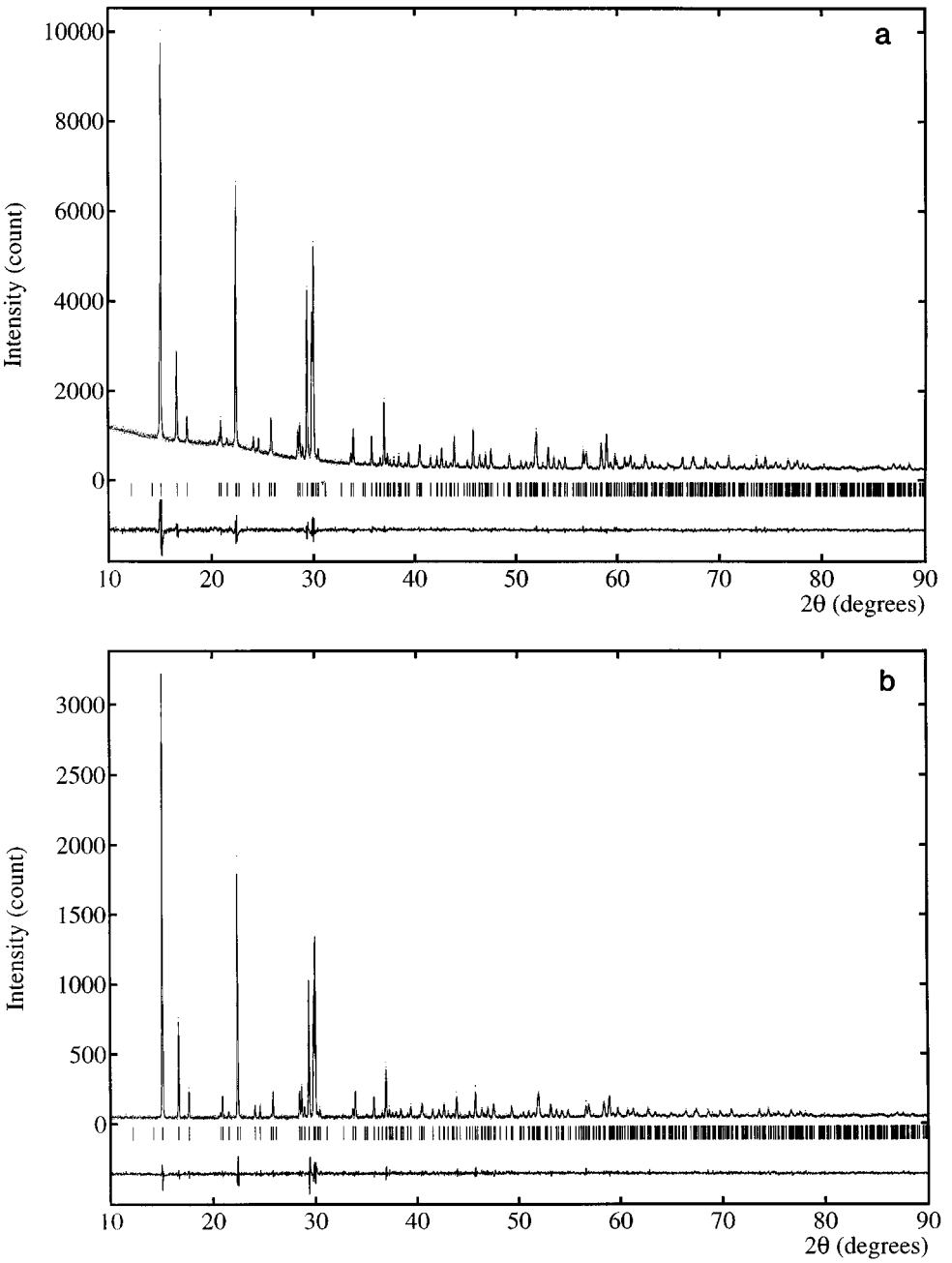

FIG. 1. Observed and final calculated profile plots, thick marks for the Bragg peak positions, and the difference profile plot from the Rietveld refinement of $NH_4VP_2O_7$: (a) with data from the STOE STADI P; (b) with data from the Siemens D500.

limited the choice of space groups to *P*4*b*2, *P*4*bm*, and *P*4/*mbm*. Additional considerations about a possible structure model, such as special positions for most of the atoms (formula units $Z = 2$, but general positions either 8 or 16) and one double bond between an oxygen and the vanadium(IV), favored the space group *P*4*bm* because it was found for the equivalent potassium compound (10).

The STADI P data were fitted by applying the pattern decomposition method proposed by Le Bail (21) with the program PROFIL (22). The refinement of the crystallographic and instrumental parameters (cell parameters, half-width, profile function etc.) led to the separation of 146 reflections with the R factors (background excluded) $R_{wp} = 14.0\%$ and $R_{exp} = 5.4\%$. A structure solution was

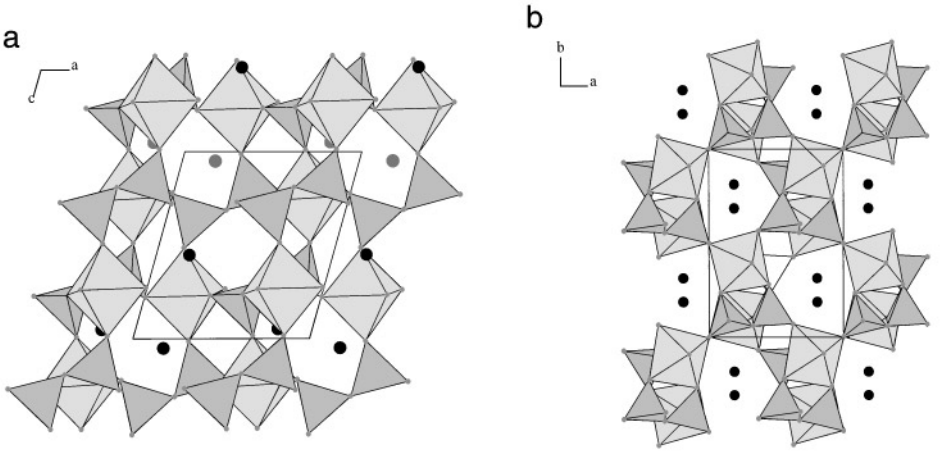

FIG. 2. Polyhedral representation of $NH_4VP_2O_7$: (a) projection along *b*; (c) projection along *c*; the light gray tetrahedra represent the PO_4 polyhedra, the black spheres, the NH_4^+ cations.

attempted by means of the direct methods of the program SHELXS-86 (23) with 87 observable reflections (corrected for polarization and Lorentz effect but not for absorption (Table 3)), and from the Fourier synthesis the positions of vanadium, phosphorus and three oxygen atoms could be deduced unambiguously. Subsequent Fourier difference syntheses with SHELXL-93 (30) and Rietveld refinement with PROFIL revealed and confirmed the missing oxygen and the nitrogen of the ammonium cation.

A comparison with $K_2VOP_2O_7$ (10) confirmed that they are isostructural to each other; in contrast to them, the Rb and Cs containing vanadyl diphosphates (31) exhibit different structures and space groups due to the different sizes of the alkali cations.

The Rietveld refinement of $(NH_4)_2VOP_2O_7$ without the H atoms led again to a negative thermal parameter for N, as was earlier described for $NH_4VP_2O_7$. The inclusion of the four H atoms in form of an ideal tetrahedron around the N atom using chemical restraints on bonds and angles resulted in a *B* value for N (Table 4) comparable to the equivalent potassium compound (10). Additionally, the intensity *R* factor dropped from around 10% down to 5.8% (Table 3).

Discrepancies in the profile fit, especially for the first two reflections at 15° (2θ) , and additional weak unindexed reflections led to the assumption of an impurity phase. Careful examination revealed the presence of $NH_4VP_2O_7$ as the second phase. From the preparation point of view, it was always difficult to prevent the formation of that second phase because of the relative small difference in the reaction conditions. The exclusion of the strongest peaks (2θ ranges: 14–17°, 22–23°, 29–30°) of that compound resulted in a better profile fit ($R_{wp} = 10.7\%$ and $R_{exp} = 6.2\%$), but the number of structure factors for the main phase was reduced and that increased the intensity *R* factor, R_I, to 7.1%. There was no change in the structure model. The upper diagram in Fig. 3 shows the Rietveld refinement neglecting the impurity, the lower one displays the exclusion of three ranges, and the lower thick marks in that diagram present the reflection positions of the impurity phase.

Data Analysis of $(NH_4)_2(VO)_3(P_2O_7)_2$

The determined crystallographic data (lattice constants, space group, etc.) for the compound $(NH_4)_2(VO)_3(P_2O_7)_2$ using the program package VISUAL X^{POW} are given in Table 5. From the crystal system and the systematic absences, the following two space groups were possible: $Pna2_1$ or *Pnam* (standard setting *Pnma*). As already discussed for the other two ammonium vanadium diphosphates, $(NH_4)_2(VO)_3(P_2O_7)_2$ is structural related to the alkali compounds $M_2(VO)_3(P_2O_7)_2$, M = K, Rb, Cs (11–13). In this case the structure is more complex than the previous two. The powder pattern as shown in Fig. 5 is characterized by an increased number of overlapping reflections and a high background in the lower 2θ range due to scattering on the capillary and absorption.

The structures $K_2(VO)_3(P_2O_7)_2$ (11) and $Rb_2(VO)_3(P_2O_7)_2$ (12) were used as starting models for Rietveld refinement. In the latter case, in the centrosymmetric space group *Pnam*, a reasonable refined structure could be obtained (Table 6). The vanadium V(3) had to be shifted away along *c* from its special position, an inversion center, and had to be described by a disorder model of two atoms and an occupancy factor of 0.5. An individual refinement of the displacement parameters of all three vanadium atoms

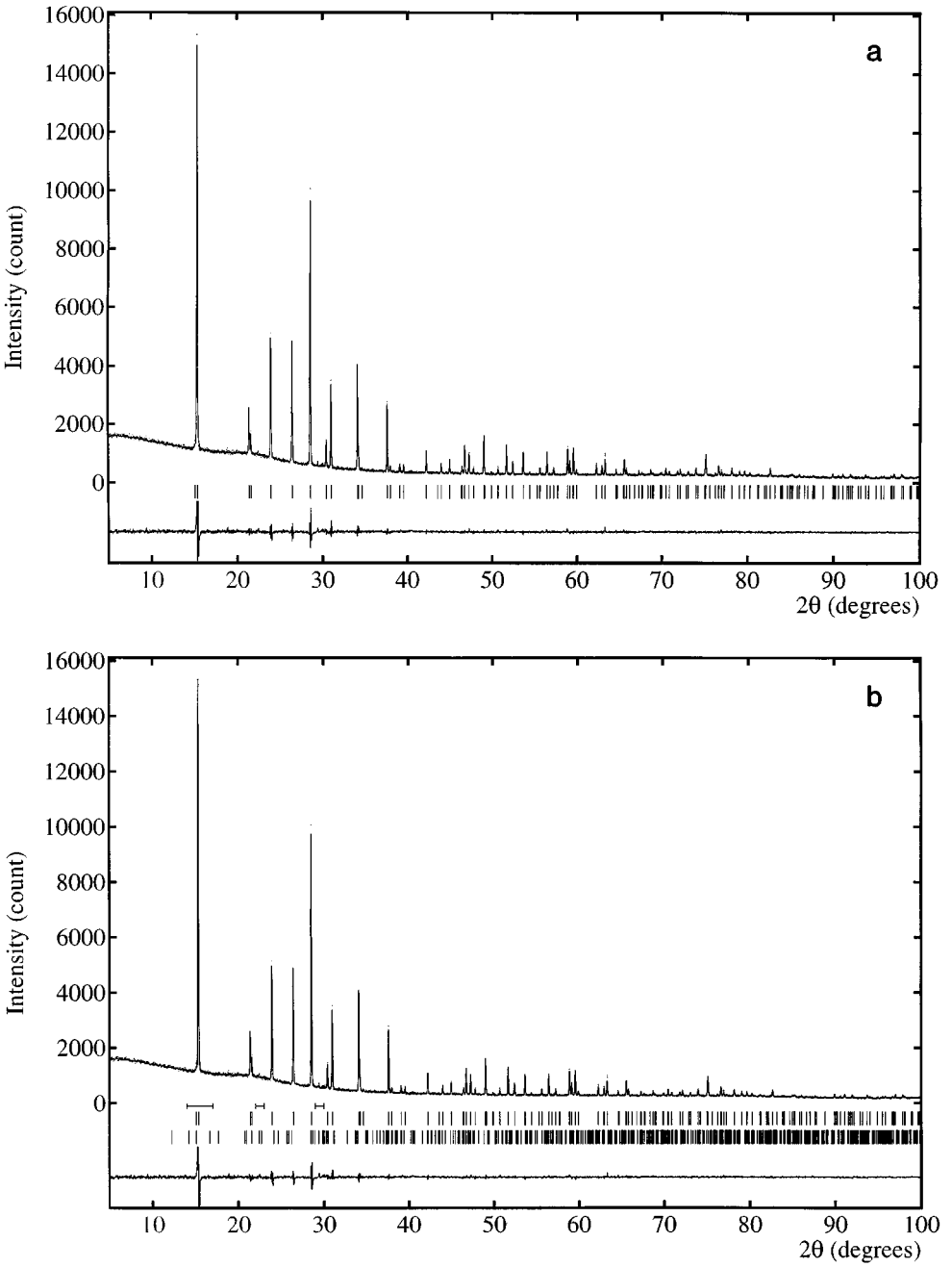

FIG. 3. Observed and final calculated profile plots, thick marks for the Bragg peak positions, and the difference profile plot from the Rietveld refinement of $(NH_4)_2$) VOP_2O_7 with STOE STADI P data: (a) whole pattern, no excluded regions; (b) three excluded ranges and lower thick marks for the Bragg peak positions of the impurity phase $NH_4VP_2O_7$.

resulted in a very high factor for V(3). Therefore this splitting of the V(3) atom position was chosen, which is also in agreement with the disorder model of the isostructural Rb_2- and $Cs_2(VO)_3(P_2O_7)_2$ (12, 13). A similar positional disorder of vanadium has been found in other vanadyl phosphates (32, 33).

The refinement with the potassium model in the noncentrosymmetric space group $Pna2_1$ led to a local minimum without a final convergence defined by the shift to an error ratio smaller than 10%. The structure model was not stable, i.e. certain bonds were either too short or too long. This was very obvious in the case of the P–O bonds where the values

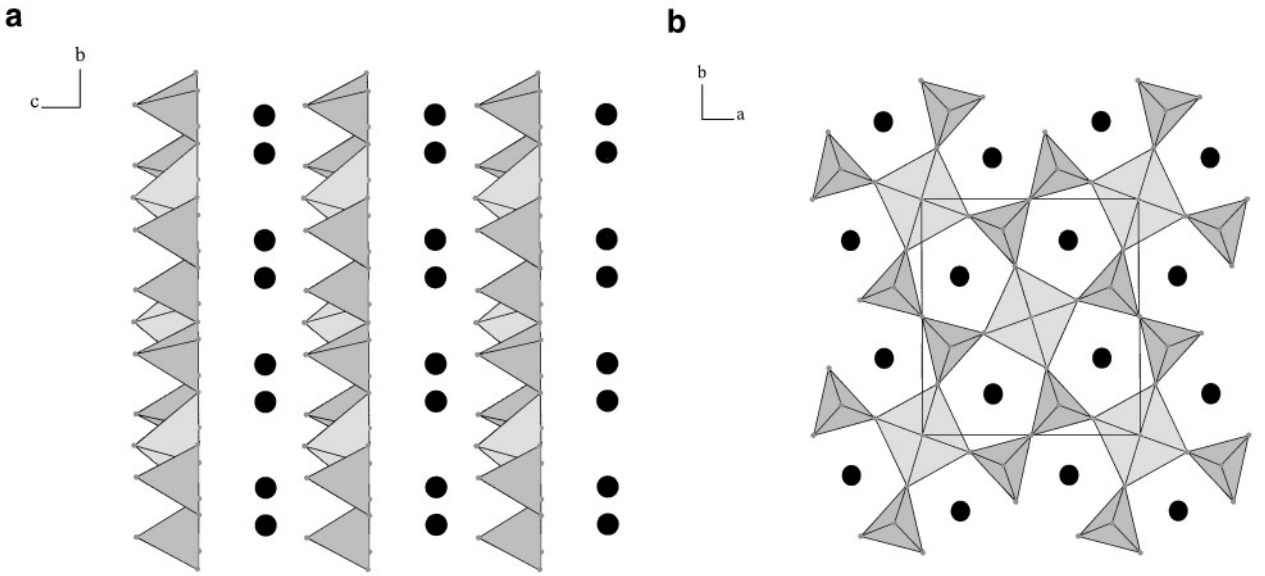

FIG. 4. $(NH_4)_2VOP_2O_7$ polyhedral representations with an unit cell: (a) projection along *a* and (b) projection along *c*; the light gray tetrahedra represent the PO_4 polyhedra, the black spheres, the NH_4^+ cations.

were in a range between 1.31 and 1.75 Å. The standard deviations for bonds and angles were more than three times higher due to the loss of symmetry constraints which increased the number of structural parameters. All atoms, which were in the centrosymmetric case related by the mirror plane perpendicular to the *c* axis, showed a high correlation with each other which prevented a convergence of the refinement.

Again, the hydrogen atoms of the NH_4^+ cations were included via geometrical constraints into the centrosymmetric model which led to positive displacement parameters ($B = 3.5$ Å^2) for the two nitrogen atoms (Table 6).

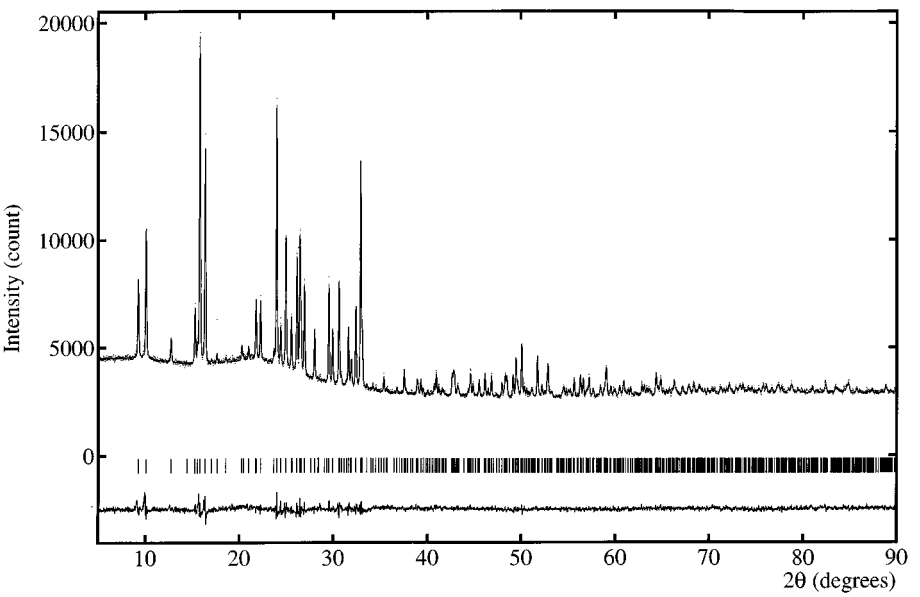

FIG. 5. Observed and final calculated profile plots, thick marks for the Bragg peak positions, and the difference profile plot from the Rietveld refinement of α-$(NH_4)_2(VO)_3P_2O_7$ with STOE STADI P data.

Structure Discussions

$NH_4VP_2O_7$

The structure $NH_4VP_2O_7$ consists of a mixed three-dimensional framework of corner-sharing $V^{III}O_6$ octahedra and PO_4 tetrahedra of the diphosphate groups (Fig. 2a,b). All figures displaying structure models are drawn with the program DIAMOND (27). Beside the isostructural compounds MVP_2O_7, with $M = K$, Rb, Cs (7–9), there is a structural relationship to molybdenum diphosphates, such as $KMoP_2O_7$ (28), and the Rb- and Cs-containing compounds (29), respectively.

The slightly distorted VO_6 octahedra are characterized by V–O distances of about 2 Å and angles close to 90 and 180°. Each PO_4 tetrahedron of a diphosphate group has one longer P–O bond (~1.6 Å) corresponding to the bridging atom of the P_2O_7 group and three shorter bonds (~1.5 Å), where the oxygen atoms are shared with the neighboring VO_6 octahedra. The values are comparable with those isostructural compounds determined from single-crystal data despite an order of magnitude higher standard deviations for atom positions and bonds, and therefore bond distances and angles are not listed in an extra table except for the N–O distances.

The structure is characterized by $[VP_2O_7]_\infty$ sheets parallel to the *xy* planes, and stacking them along the *c* direction leads to heptagonal channels (Fig. 2b). Additionally, there are hexagonal-shaped channels along the [110] direction and the two tetrahedra of a P_2O_7 group are in a nearly staggered configuration. All these features have been already described in more detail in the case of the isostructural compounds $KMoP_2O_7$ (28) and $CsMoP_2O_7$ (29).

The positions of the NH_4^+ cations are within these channels or tunnels with ten oxygen atoms as nearest neighbors in a range between 2.86 and 3.34 Å (Table 7). The K–O distances in the isostructural potassium compound (7) ranging from 2.759 to 3.255 Å are slightly smaller whereas the Rb–O distances of the rubidium structure (8) with values between 2.859 and 3.318 Å are comparable with the N–O distances. The greater mobility of these ammonium ions within the channels corresponds with their relatively large displacement factors (Table 2) and with the values found in other isostructural compounds (7–9, 28, 29). This also implies that possible additional hydrogen bonds to the nearest oxygen neighbors are too weak to exert an effect on the high displacement factor of the NH_4^+ cation.

$(NH_4)_2VOP_2O_7$

The structure model of $(NH_4)_2VOP_2O_7$ (H atoms are not displayed) is shown in Fig. 4, which consists of planar layers of vanadyl diphosphates and NH_4^+ in between. The layers are made up of corner-sharing VO_5 pyramids and PO_4 tetrahedra, with the quadratic basal plane and one triangular plane, respectively, parallel to (001). The four oxygen atoms of the basal plane of a VO_5 pyramid are from four different diphosphate groups. The apical oxygen O(1) is double-bonded to vanadium. Its bonding distance of 1.61 Å is unequivocally shorter than the distance between vanadium and the other oxygen atoms (1.98 Å). This is in good agreement with the local coordination of other vanadyl diphosphates containing potassium, rubidium, or cesium despite differences in the overall structure. A similar agreement can be found for the P–O bonding within the diphosphate groups. The distance between the bridging oxygen O(4) and phosphorus is with 1.60 Å significantly longer than the other P–O bonds (~1.50 Å).

Linking of two VO_5 pyramids via two tetrahedra of one P_2O_7 group and another tetrahedron of a second P_2O_7 group within a layer leads of pentagonal windows (Fig. 4b). The regular stacking of these sheets along the *c* direction extends the windows to pentagonal channels. The distance between the layers corresponds to the lattice constant *c* (5.7658 Å).

The NH_4^+ cations are located between the vanadyl phosphate layers within the channels on mirror planes and link neighboring sheets through their tenfold coordination with the oxygen atoms from these layers (N–O distances in a range between 2.71 and 3.34 Å, see Table 7). The shortest NH_4^+–NH_4^+ distances are 4.09 Å and are comparable with K^+–K^+ at 4.00 Å. The K–O distances are slightly smaller,

TABLE 7
Selected Interatomic N–O Distances (Å) (Rietveld Refinement with Data from STOE STADI P)

	$NH_4VP_2O_7$		
N–O(1)	3.34(3)	N–O(5)	3.24(3)
N–O(2)	3.12(2)	N–O(5)	3.10(2)
N–O(3)	2.96(3)	N–O(6)	3.04(3)
N–O(3)	2.98(3)	N–O(6)	2.86(3)
N–O(4)	2.83(3)	N–O(7)	3.24(2)
	$(NH_4)_2VOP_2O_7$		
N–O(1)	3.34(2)	N–O(3)	3.11(3)
N–O(1)	3.34(2)	N–O(3)	3.17(3)
N–O(2)	2.71(3)	N–O(3)	3.17(3)
N–O(2)	2.90(3)	N–O(3)	3.11(3)
N–O(2)	2.90(3)	N–O(4)	3.08(3)
	$(NH_4)_2(VO)_3(P_2O_7)_2$		
N(1)–O(2)	3.08(3)	N(1)–O(4)	3.19(2)
N(1)–O(3)	3.25(2)	N(1)–O(5)	3.31(3)
N(1)–O(3)	3.25(2)	N(1)–O(5)	3.31(3)
N(1)–O(4)	3.19(2)	N(1)–O(6)	3.12(3)
		N(1)–O(11)	3.10(3)
N(2)–O(3)	3.31(3)	N(2)–O(7)	2.83(2)
N(2)–O(3)	3.31(3)	N(2)–O(7)	2.83(2)
N(2)–O(4)	3.37(2)	N(2)–O(8)	3.07(2)
N(2)–O(4)	3.37(2)	N(2)–O(8)	3.07(2)
		N(2)–O(10)	3.13(3)

between 2.677 and 3.311 Å. Therefore both compounds are isostructural and consist of planar layers of vanadyl diphosphates. The equivalent Rb^+ and Cs^+ containing compounds (31) have larger distances between their alkali ions with 4.38 Å for Rb^+ and 4.52 Å for Cs^+. The layers are corrugated and the channels have a heptagonal shape.

$(NH_4)_2(VO)_3(P_2O_7)_2$

Representations of the structure in projections along the *b* and *c* axes are given in Fig. 6. The compound $(NH_4)_2(VO)_3(P_2O_7)_2$ consists of a three-dimensional framework of corner-sharing VO_5 pyramids, VO_6 octahedra, and PO_4 tetrahedra and intersecting channels along the *b* and *c* axes, where the NH_4^+ cations are located on mirror planes.

There are three crystallographic distinct VO_x polyhedra. V(1) in a square pyramidal VO_5 coordination and V(2) in a stretched octahedral VO_6 coordination, assuming that the apical oxygen O(10) from VO_5 is at a distance of 2.49 Å still weakly coordinated to V(2), form V_2O_{10} units, which are connected via PO_4 tetrahedra with the neighboring chains of VO_6 octahedra of V(3) as displayed in Fig. 6. These links of polyhedra within planes perpendicular to the axes *c* and *b* delimit windows, the stacking of them along these axes leads to the intersecting channels.

The largest channel along the *c* direction (Fig. 6b) is delimited by the edges of a V_2O_{10} unit, another V(2) O_6 octahedron, a V(3)O_6 octahedron, and three PO_4 tetrahedra. Two smaller windows are due to the connection of two V_2O_{10} units and two PO_4 tetrahedra in one case and the linking of a V(1)O_5 pyramid, a V(3)O_6 octahedron, and two PO_4 tetrahedra in the second case.

Along the *b* axis the channels are formed by the alternating stacking of heptagonal and pentagonal rings, as has been described for the isostructural alkali compounds (11–13).

The position of vanadium in its coordination polyhedra is shifted off the center due to the double bond to one of the oxygen atoms forming the vanadyl group. All three crystallographic distinct VO_x polyhedra are characterized by one short apical V=O bond at about 1.60 Å which is comparable to other vanadium (IV, V) oxides (11,13). The other V–O bonds are in a range between 1.93 and 2.07 Å except for V(2)–O(10) with 2.49 Å. The V(3) octahedra are linked with each other via alternating short and long bonds to O(9) with distances of 1.60 and 2.07 Å, respectively. The way of the alternating bonds depends on the described disorder model for V(3) and is mainly along the *c* axis which is also the direction of the V(3)O_6 octahedral chains (Fig. 6a).

The PO_4 tetrahedra of the diphosphate groups are characterized by three shorter bonds in the range between 1.46 and 1.52 Å and a longer one with 1.60 or 1.61 Å, respectively, the latter represents the bonding of the phosphorus atoms to the bridging oxygen atoms. These values are comparable

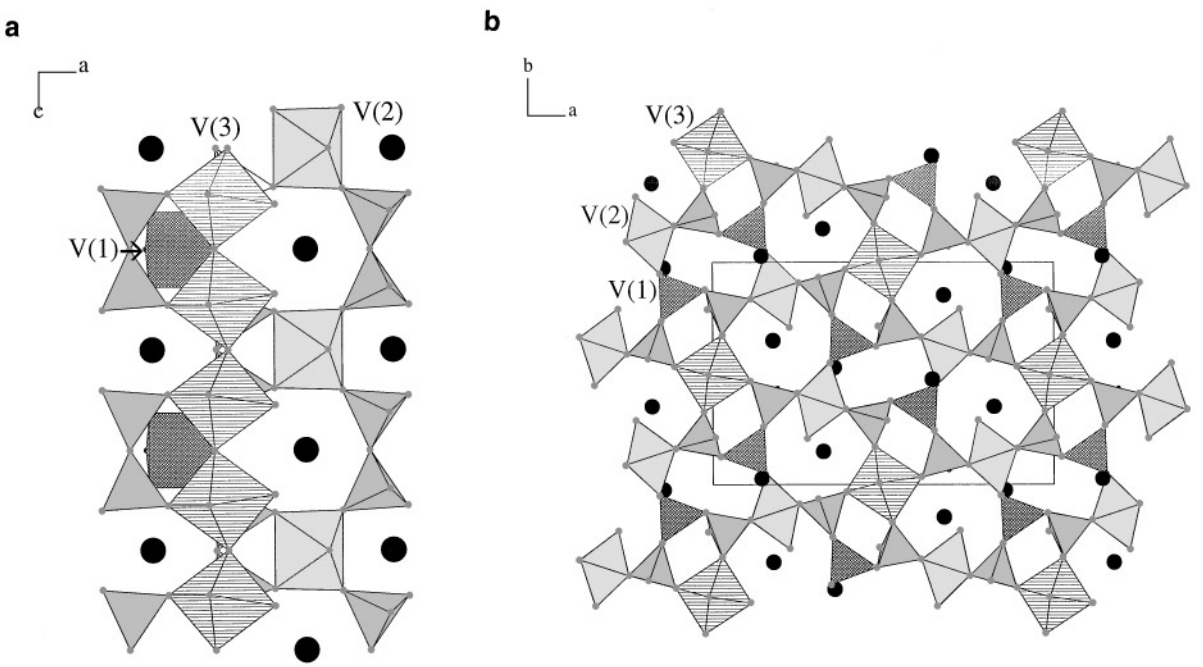

FIG. 6. α-$(NH_4)_2(VO)_3P_2O_7$ (a) polyhedral representation of the V(3) O_6 octahedra chain, projection along the *b* axis; (b) projection of the structure along *c*; the light gray tetrahedra represent the PO_4 polyhedra, the black spheres, the NH_4^+ cations.

to the corresponding Rb and Cs vanadyl diphosphates (12, 13). The K compound (11) in this comparison departs from this rule because the bridging oxygen O(17) of the first P_2O_7 group has P–O bonds of 1.54(8), which is only the second longest bond of the $P(1)O_4$ tetrahedron, and 1.63(8) Å, which is the longest bond of the $P(2)O_4$ tetrahedron. The reason for that may be due to the small number of measured reflections, missing absorption correction or even the uncertainty in the correct space group which may also explain the high standard deviations of the bond lengths.

The closest coordination distances for the two crystallographic distinct NH_4^+ cations to the surrounding oxygen atoms are between 3.08 and 3.31 Å for N(1) and between 2.83 and 3.37 Å for N(2) (Table 7). Again, the Rb^+ cations have similar coordination distances to 9 neighboring oxygens with values between 3.062 and 3.357 Å for Rb(1) and 2.930 and 3.336 Å for Rb(2). Whereas the Cs has larger bond lengths, with Cs(1) surrounded by 13 oxygens between 3.167 and 3.530 Å, and Cs(2) by 11 oxygens between 3.071 and 3.489 Å. Potassium is characterized by shorter K–O distances for K(1) with 8-fold coordination in the range between 2.66 and 3.33 Å and for K(2) with 7-fold coordination between 2.99 and 3.28 Å.

All of these cations are located in the channels of the framework structure and show in comparison to the other atoms of the structure a higher mobility and consequently higher displacement parameters (Table 6).

CONCLUSIONS

The structures of the three ammonium vanadium diphosphates have been studied by means of X-ray powder diffraction because no suitable single crystals could be prepared. The analysis of the three different compounds underlines the great structural variety of the vanadium phosphorus oxides due to the flexibility in the arrangement of VO_x polyhedra and PO_4 tetrahedra. The results of the structure determinations show that the ammonium samples are isostructural to corresponding alkali compounds. Despite a lower precision and accuracy of the structure models derived from the Rietveld refinement of the powder data compared to the single-crystal values of the alkali vanadium diphosphates, the same bonding characteristics, e.g. short double bonds of the vanadyl group, reasonable P–O distances for the P_2O_7 groups could be obtained.

The negative displacement parameter for the nitrogen atoms of the NH_4^+ cations in all three compounds was not caused by errors in the data but was due to the missing of the hydrogen positions; therefore the positions were included via geometrical restraints to form an ideal tetrahedron. For the purpose of comparison a powder data set for $NH_4VP_2O_7$ was collected on a Siemens Bragg–Brentano diffractometer D500, and the same effect (a negative thermal parameter for N; H positions not included) was observed. As already mentioned, the determination of thermal factors using X-ray powder data are generally less accurate. In the case of the transmission data (STOE STADI P), an absorption correction is required, but other factors, such as background determination and monochromator correction, may also affect the displacement parameters. At least relative differences in these parameters depending on the atom type, e.g. high values for the NH_4^+ cations, can be ascertained.

Because of these high displacement parameters, the hydrogens are disordered around the nitrogen, and low temperature studies may help to reduce possible dynamic disorder and establish a model of hydrogen bonding of the NH_4^+ cations, as has been done in the case of β-$(NH_4)_2FeF_5$ (34).

The comparison of the reflection data with the transmission data yielded for both a similar good structure model, but the precision based on the estimated standard deviations is too optimistic. The profile fit for the Bragg–Brentano data set is slightly better than in the transmission case.

The ambiguity in the choice of the space group $Pna2_1$ or *Pnam* for the last structure α-$(NH_4)_2(VO)_3(P_2O_7)_2$ could not be resolved, but the centrosymmetric setting led to convergence in the Rietveld refinement. In the noncentrosymmetric case, no disorder model for the V(3) is required but there is no final convergence and the structure breaks up (e.g. unusual P–O bonds) because of high correlations between formerly symmetry-related atoms. The pair of such common space groups $Pna2_1$–*Pnam* is a typical example where systematic absences are no help, and results from *E* statistics based on powder data are doubtful. Following the comments by R. E. Marsh (35, 36) and from the results above, the space group *Pnam* (standard setting *Pnma*) should be preferred.

The knowledge of the structure for the as-synthesized α-$(NH_4)_2(VO)_3(P_2O_7)_2$ can be used to study the structure of α-$(NH_4)_2(VO)_3(P_2O_7)_2$ generated by the transformation of vanadium phosphates under ammoxidation conditions (methyl aromatic compound, ammonia, air, water vapor) (6).

ACKNOWLEDGMENTS

The authors thank Dr. J. K. Cockcroft and Mr. M. Vickers, Industrial Materials Group, Department of Crystallography, Birkbeck College, University of London, for the opportunity to collect a Siemens D500 powder data set for $NH_4VP_2O_7$, for the Rietveld program PROFIL (author, J. K. Cockcroft), and for helpful discussions. Financial support by the Bundesministerium für Bildung, Wissenschaft, Forschung und Technologie, the Berliner Senat, Senatsverwaltung für Wissenschaft, Forschung und Kultur (Project No. 03C3005), and the International Centre for Diffraction Data (ICDD) are gratefully acknowledged.

REFERENCES

1. J. W. Johnson, D. C. Johnston, A. J. Jacobson, and J. F. Brody, *J. Am. Chem. Soc.* **106,** 8123 (1984).

2. A. Martin, B. Lücke, H. Seeboth, G. Ladwig, and E. Fischer, *React. Kinet. Catal. Lett.* **38,** 33 (1989).
3. A. Martin, B. Lücke, G.-U. Wolf, and M. Meisel, *Catal. Lett.* **33,** 349 (1995).
4. A. Martin, B. Lücke, B. Seeboth, and G. Ladwig, *Appl. Catal.* **49,** 205 (1989).
5. Y. Zhang, A. Martin, G.-U. Wolf, S. Rabe, H. Worzala, B. Lücke, M. Meisel, and K. Witke, *Chem. Mater.* **8,** 1135 (1996).
6. L. Wilde, U. Steinike, A. Martin, G.-U. Wolf, and B. Lücke. [In preparation]
7. L. Benhamada, A. Grandin, M. M. Borel, A. Lecclaire, and B. Raveau, *Acta Crystallogr. C* **47,** 424 (1991).
8. U. Flörke, *Z. Kristallogr.* **191,** 139 (1990).
9. Y. P. Wang and K. H. Lii, *Acta Crystallogr. C* **45,** 1210 (1989).
10. Y. E. Gorbunova, S. A. Linde, A. V. Larov, and I. V. Tananaev, *Dokl. Akad. Nauk SSSR* **250**(2), 350 (1980).
11. A. Leclaire, H. Chahboun, D. Groult, and B. Raveau, *J. Solid State Chem.* **77,** 170 (1988).
12. K. H. Lii, Y. P. Wang, C. Y. Cheng, S. L. Wang, and H. C. Ku, *J. Chin. Chem. Soc.* **37,** 141 (1990).
13. K. H. Lii, Y. P. Wang, and S. L. Wang, *J. Solid State Chem.* **80,** 127 (1989).
14. H. M. Rietveld, *J. Appl. Crystallogr.* **2,** 65 (1969).
15. A. Le Bail, G. Ferey, P. Amoros, and D. Beltran-Porter, *Eur. J. Solid State Inorg. Chem.* **26,** 419 (1989).
16. A. Le Bail, G. Ferey, P. Amoros, D. Beltran-Porter, and G. Villeneuve, *J. Solid State Chem.* **79,** 169 (1989).
17. R. G. Teller, P. Blum, E. Kostiner, and J. A. Hriljac, *J. Solid State Chem.* **97,** 10 (1992).
18. K. Schlesinger, late draft of dissertation (1983).
19. D. B. Wiles and R. A. Young, *J. Appl. Cryst.* **14,** 149 (1981).
20. STOE & CIE GmbH, "VISUAL X^{POW}: Software package for the STOE POWDER DIFFRACTION SYSTEM (STADI P)." Darmstadt, Germany, 1994.
21. A. Le Bail, H. Duroy, and J. L. Fourquet, *Mater. Res. Bull.* **23,** 447 (1988).
22. J. K. Cockcroft, "PROFIL: A Rietveld Program for the Simultaneous Refinement of Crystal Structures from Several Single- or Multi-Phase Powder, Neutron and Synchrotron Radiation Diffraction Data Sets or Pattern Decomposition Thereof," Version 5.17. Birkbeck College, London (1994).
23. G. M. Sheldrick, *Acta Crystallogr. A* **46,** 467 (1990).
24. R. A. Young, "The Rietveld Method" (R. A. Young, Ed.), p. 1–39. Oxford Univ. Press, Oxford, 1993.
25. P. Thompson and I. G. Wood, *J. Appl. Crystallogr.* **16,** 458 (1983).
26. "International Tables for X-ray Crystallography," Vol. III. Kynoch Press, Birmingham, UK, 1968.
27. G. Bergerhoff, "Diamond: Visuelles Informationsystem für Kristallstrukturen." Gerhard-Domagk-Str. 1, 53121 Bonn, Germany, 1995.
28. A. Leclaire, M. M. Borel, A. Grandin, and B. Raveau, *J. Solid State Chem.* **78,** 220 (1989).
29. K. H. Lii and R. C. Haushalter, *Acta Crystallogr. Sect. C* **43,** 2036 (1987).
30. G. M. Sheldrick, "SHELXL-93: A program for the refinement of crystal structures." University of Göttingen, Germany, 1993.
31. K. H. Lii and S. L. Wang, *J. Solid State Chem.* **82,** 239 (1989).
32. K. H. Lii, H. J. Tsai, and S. L. Wang, *J. Solid State Chem.* **87,** 396 (1990).
33. R. G. Teller, P. Blum, E. Kostinger, and J. A. Hriljac, *J. Solid State Chem.* **97,** 10 (1992).
34. L. Croguennec, P. Deniard, R. Brec, M. Couzi, C. Sourisseau, J. L. Fourquet, and Y. Calage, *J. Solid State Chem.* **131,** 189 (1997).
35. R. E. Marsh, *Acta Crystallogr. B* **42,** 193 (1986).
36. R. E. Marsh, *Acta Crystallogr. B* **51,** 897 (1995).